

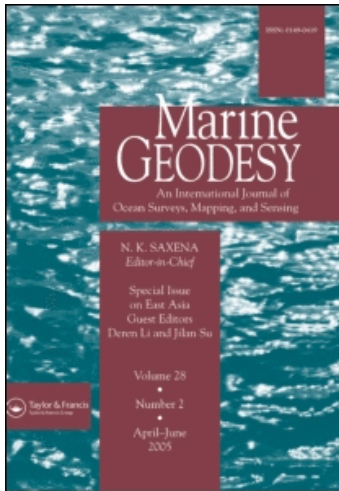
This article was downloaded by: [Ohio State University Libraries]

On: 12 August 2009

Access details: Access Details: [subscription number 907133608]

Publisher Taylor & Francis

Informa Ltd Registered in England and Wales Registered Number: 1072954 Registered office: Mortimer House, 37-41 Mortimer Street, London W1T 3JH, UK



Marine Geodesy

Publication details, including instructions for authors and subscription information:

<http://www.informaworld.com/smpp/title-content=t713657895>

Helmand River Hydrologic Studies Using ALOS PALSAR InSAR and ENVISAT Altimetry

Zhong Lu ^a; Jin-Woo Kim ^b; Hyongki Lee ^b; C. K. Shum ^b; Jianbin Duan ^b; Motomu Ibaraki ^b; Orhan Akyilmaz ^c; Chung-Hye Read ^d

^a U.S. Geological Survey, Vancouver, Washington, USA ^b School of Earth Sciences, The Ohio State University, Columbus, Ohio, USA ^c Department of Geodesy and Photogrammetry, Istanbul Technical University, Istanbul, Turkey ^d Basic and Applied Research Office, InnoVision, National Geospatial-Intelligence Agency, Bethesda, Maryland, USA

Online Publication Date: 01 July 2009

To cite this Article Lu, Zhong, Kim, Jin-Woo, Lee, Hyongki, Shum, C. K., Duan, Jianbin, Ibaraki, Motomu, Akyilmaz, Orhan and Read, Chung-Hye(2009)'Helmand River Hydrologic Studies Using ALOS PALSAR InSAR and ENVISAT Altimetry',Marine Geodesy,32:3,320 — 333

To link to this Article: DOI: 10.1080/01490410903094833

URL: <http://dx.doi.org/10.1080/01490410903094833>

PLEASE SCROLL DOWN FOR ARTICLE

Full terms and conditions of use: <http://www.informaworld.com/terms-and-conditions-of-access.pdf>

This article may be used for research, teaching and private study purposes. Any substantial or systematic reproduction, re-distribution, re-selling, loan or sub-licensing, systematic supply or distribution in any form to anyone is expressly forbidden.

The publisher does not give any warranty express or implied or make any representation that the contents will be complete or accurate or up to date. The accuracy of any instructions, formulae and drug doses should be independently verified with primary sources. The publisher shall not be liable for any loss, actions, claims, proceedings, demand or costs or damages whatsoever or howsoever caused arising directly or indirectly in connection with or arising out of the use of this material.

Helmand River Hydrologic Studies Using ALOS PALSAR InSAR and ENVISAT Altimetry

ZHONG LU,¹ JIN-WOO KIM,² HYONGKI LEE,² C. K. SHUM,²
JIANBIN DUAN,² MOTOMU IBARAKI,²
ORHAN AKYILMAZ,³ AND CHUNG-HYE READ⁴

¹U.S. Geological Survey, Vancouver, Washington, USA

²School of Earth Sciences, The Ohio State University, Columbus, Ohio, USA

³Department of Geodesy and Photogrammetry, Istanbul Technical University,
Istanbul, Turkey

⁴Basic and Applied Research Office, InnoVision, National
Geospatial-Intelligence Agency, Bethesda, Maryland, USA

The Helmand River wetland represents the only fresh-water resource in southern Afghanistan and one of the least mapped water basins in the world. The relatively narrow wetland consists of mostly marshes surrounded by dry lands. In this study, we demonstrate the use of the Advanced Land Observing Satellite (ALOS) Phased Array type L-band Synthetic Aperture Radar (PALSAR) Interferometric SAR (InSAR) to detect the changes of the Helmand River wetland water level. InSAR images are combined with the geocentric water level measurements from the retracked high-rate (18-Hz) Environmental Satellite (Envisat) radar altimetry to construct absolute water level changes over the marshes. It is demonstrated that the integration of the altimeter and InSAR can provide spatio-temporal measurements of water level variation over the Helmand River marshes where in situ measurements are absent.

Keywords Helmand River, water level change, InSAR, satellite altimetry

1. Introduction

The Helmand River is the lifeblood of southern Afghanistan. It drains about 40% of Afghanistan's fresh water, which is primarily provided by melting snow and storm runoff (Vining and Vecchia 2007). The Helmand River basin is the largest in Afghanistan and covers the southern half of the country. Due to the desert environment, the water level variation of the Helmand River is characterized by large fluctuations owing to flood and drought (Williams-Sether 2008). The extreme drought in the basin since 1999 has caused socio-economic problems which threaten the livelihood of those interlinked with the wetland products and services. This drought also has caused environmental problems, resulting in the destruction of natural ecological systems. The desperate situation around the Helmand River basin requires an improvement in the management of restricted water and water

Received 10 February 2009; revised and accepted 4 June 2009.

Address correspondence to Hyongki Lee, School of Earth Sciences, The Ohio State University, 275 Mendenhall Laboratory, 125 South Oval Mall, Columbus, OH 43210. E-mail: lee.2444@osu.edu

monitoring to prevent the abrupt flooding by the heavy rains, which have occasionally occurred in 2005 and 2007 (ReliefWeb 2003; Integrated Regional Information Networks 2005). However, we have poor knowledge of the spatial and temporal dynamics of the surface water storage change over the region. In this study, we utilize satellite radar remote sensing technologies, which provide useful measurements to monitor the spatial and temporal variations of water level over the region. This study also intends to show how active remote sensing techniques could provide hydrologic measurements in one of the least mapped bodies of water in the world.

Interferometric Synthetic Aperture Radar (InSAR) has been proven to be useful in measuring centimeter-scale water level changes over the Amazon flood plain using L-band Shuttle Imaging Radar-C (SIR-C) and Japanese Earth Resources Satellite 1 (JERS-1) imagery (Alsdorf et al. 2000, 2001), and over the Everglades wetland in Florida using the L-band JERS-1 data (Wdowinski et al. 2004). Furthermore, European Remote-sensing Satellite (ERS)-1/2 C-band images have been used to study water level changes over the Louisiana wetlands (Lu et al. 2005; Lu and Kwoun 2008). The usefulness of these techniques is based on the fact that the water beneath the swamp forest can provide double-bounce scattering, which allows interferogram coherence to be maintained. However, the wetlands in the Helmand River basin are relatively narrow and covered mostly with marshes, not swamp forests, and surrounded by dry lands.

Over the past few years, satellite radar altimetry has been successfully used for water level monitoring over large inland water bodies such as the Great Lakes (Morris and Gill 1994; Birkett 1995) and the Amazon basin (Birkett 1998; Birkett et al. 2002), which have higher chances to be processed as ocean-like return. However, a significant amount of data loss can occur during the periods of stage minima (lowest water level) due to the interruptions to the water surface by the surrounding topography. Furthermore, the radar return from a relatively small water body can be distorted. These limitations can be partially overcome by retracking individual return waveform (Berry et al. 2005; Frappart et al. 2006; Lee et al. 2009). In this study, we utilize the Environmental Satellite (Envisat) 18-Hz regional stackfile (Lee et al. 2008, 2009) to carefully select individual radar return from the narrow intersection between the Helmand River and the satellite ground track. In addition, the geocentric water level changes obtained from the altimetry are used to resolve the integer ambiguity, inherent in the wrapped differential interferogram images, over the marshes of the Helmand River basin.

2. Data

In this study, 22 pairs of Advanced Land Observing Satellite (ALOS) Phased Array type L-band Synthetic Aperture Radar (PALSAR) scenes are processed, and their temporal baselines, perpendicular baselines, and dates of acquisition are given in Table 1. The pairs are composed of five paths from 548 to 552 (white boxes in Figure 1) covering the Helmand River. All scenes have an incidence angle of about 38.7° . The critical baselines of PALSAR at this incidence angle over flat terrains are about 13.1 km in Fine Beam Single-polarization (FBS) mode and 6.5 km in Fine Beam Double-polarization (FBD) mode (Sandwell et al. 2008), so we use the pairs which have the perpendicular baselines much smaller than the critical baselines (Table 1). In addition, we use SAR pairs with temporal baselines shorter than 365 days to minimize the temporal decorrelation. Because horizontal-transmit and horizontal-receive (HH) polarized SAR images maintain better coherence over wetlands than vertical-transmit and vertical-receive (VV) polarized SAR

Table 1
Temporal and perpendicular baselines of the InSAR pairs

Pair	Master date	Slave date	Path	Temporal baseline (days)	Perpendicular baseline (m)
1	2/1/2007	6/19/2007	548	138	577.3672
2	12/20/2007	3/21/2008	548	92	647.2835
3	3/21/2008	5/6/2008	548	46	563.9113
4	6/19/2007	9/19/2007	548	92	238.2067
5	9/19/2007	12/20/2007	548	92	448.6133
6	1/3/2007	2/18/2007	549	46	1880.9237
7	2/18/2007	10/6/2007	549	230	847.9038
8	1/6/2008	2/21/2008	549	46	684.1591
9	2/21/2008	4/7/2008	549	46	399.1095
10	12/5/2006	1/20/2007	550	46	-1855.0964
11	1/20/2007	6/7/2007	550	138	1755.5261
12	12/8/2007	1/23/2008	550	46	325.7641
13	1/23/2008	4/24/2008	550	92	1115.3426
14	6/7/2007	9/7/2007	550	92	653.8656
15	9/7/2007	12/8/2007	550	92	349.0772
16	12/22/2006	6/24/2007	551	184	1298.62
17	2/9/2008	5/11/2008	551	92	518.7769
18	6/24/2007	2/9/2008	551	230	1328.7804
19	1/11/2008	2/26/2008	552	46	456.9851
20	2/26/2008	5/28/2008	552	92	134.1137
21	7/11/2007	10/11/2007	552	92	539.0023
22	10/11/2007	1/11/2008	552	92	449.0074

images (Lu and Kwoun 2008), only HH polarized PALSAR images are used in this study. To remove the topographic phase, a 30-m resolution Shuttle Radar Topography Mission (SRTM) Digital Elevation Model (DEM) is used. The voids in the DEM are interpolated based on the neighborhood pixels.

The Envisat altimeter data used in this study are from September 2002 to July 2008. The Envisat orbits on a 35-day repeat cycle with 98.5° inclination. The Envisat Geophysical Data Record (GDR) contains 18-Hz retracked measurements, which have a ground spacing of approximately 350 m, and uses four different retrackers, which are OCEAN, ICE-1, ICE-2, and SEA ICE retrackers (Benveniste 2002). The instrument corrections, media corrections (dry troposphere correction, wet troposphere correction calculated by the French Meteorological Office (FMO) from the European Centre for Medium-Range Weather Forecasts (ECMWF) model, and the ionosphere correction based on Global Ionosphere Maps (GIM)), and geophysical corrections (solid Earth and pole tide) have been applied. The ionosphere corrections usually obtained by combining the dual-frequency altimeter measurement over ocean could not be used in this study because of land contaminations. Thus, the GIM ionosphere corrections, based on Total Electron Content (TEC) grids, in the GDR are used for this study. In addition, the 5.6 m level Ultra Stable Oscillator (USO) anomalies for Envisat cycles 44–70 are corrected using the European Space Agency's (ESA) correction tables (J. Benveniste, personal communications 2007).

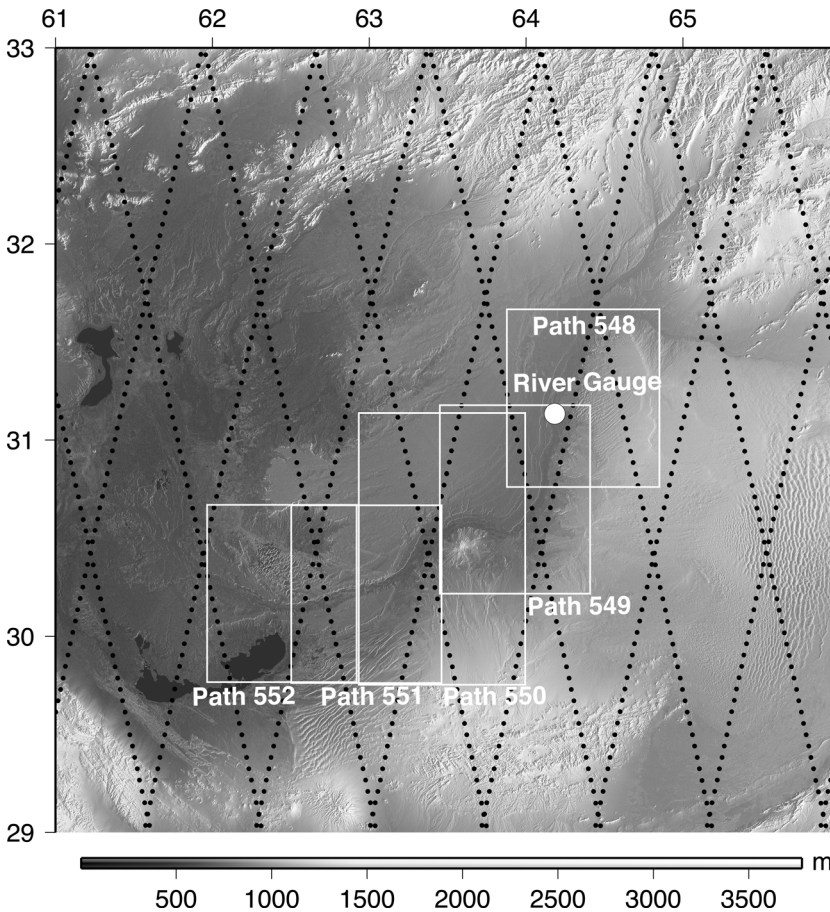


Figure 1. The Helmand River basin with the PALSAR coverage (white boxes) and 1-Hz nominal Envisat altimetry ground tracks (black dots). The white circle shows the location of the river gauge and background is the SRTM DEM.

3. Methodology

The two-pass differential InSAR method uses two SAR images acquired at different times over the same area to produce an interferogram. The phase difference of two SAR images, or interferometric phase, (ϕ), includes the signatures by topography (ϕ_{topo}), displacement (ϕ_{disp}), atmosphere effect (ϕ_{atmo}), and noise (ϕ_{noise}):

$$\phi = \phi_{topo} + \phi_{disp} + \phi_{atmo} + \phi_{noise} \quad (1)$$

The phase difference by displacement is obtained by removing other components through simulating topographic phase from DEM. The noise level of the interferometric phase depends on the coherence of the image pairs. The volumetric and surface scatterings over forested areas render low coherence or decorrelation (lost of coherence). In the case of the double-bounce backscattering, which is reflected twice from the water and tree trunks, it is possible to obtain a good coherence over swamp forests (Lu and Kwoun 2008). Over marshes comprising various species of grasses, the double-bounce backscattering may still

exist, but it depends on the water level. While the primary scattering mechanism is the volume scattering when the water level is low, specular scattering dominates when the water level is high. Therefore, the double-bounce backscattering may only occur in the intermediate range of water level. After the topographic signatures are removed, the differential interferogram is still wrapped as modulo of 2π . We must unwrap the interferogram phases to obtain actual displacement values. The marsh regions rarely have a good coherence, and thus it is difficult to do phase unwrapping (resolving the integer ambiguity, N). Therefore, in this study we use only a few high-coherence patches within the marshes. The unwrapped phase can be written as:

$$\phi_{unwrapped} = \phi - \phi_{topo} = 2\pi \cdot N + \phi_{frac} + e \quad (2)$$

where $\phi_{unwrapped}$ is the phase value after removing only the topographic phase (ϕ_{topo}) from the interferometric phase (ϕ) in Eq. (1), ϕ_{frac} is the wrapped phase value, and e is phase error term caused by the noise and atmospheric effects. What we can obtain from an interferogram is the term $\phi_{frac} + e$. To solve the integer ambiguity (N) in Eq. (2), we use the water level changes measured from the Envisat altimeter. This requires at least one patch of high-coherence pixels over which the Envisat altimeter passes. After resolving the integer ambiguity, the absolute water level changes over the coherent pixels in the interferogram can be estimated such as:

$$\hat{\phi}_{unwrapped} = -\frac{4\pi \cdot \Delta h \cdot \cos \theta_{inc}}{\lambda} \quad (3)$$

where λ is the radar wavelength (23.6 cm for L-band PALSAR), θ_{inc} is the SAR incidence angle, and $\theta_{unwrapped}$ is the unwrapped interferometric phase after the integer ambiguity is resolved.

In order to carefully select the valid 18-Hz Envisat measurements along the intersection between the Helmand River and the satellite ground track, a regional 18-Hz Envisat stackfile is developed (for details, see Lee et al. 2008, 2009). The individual 18-Hz retracked measurements using the ICE-1 retracker (Bamber 1994) with the backscattering coefficient larger than 20 dB along the intersection are spatially averaged to construct the geocentric water level change (Δh) time series.

4. Results

4.1. Water Level Change from Envisat Altimetry

As can be seen from Figure 2, the Helmand River is surrounded by mountainous regions, and the radar return can be contaminated by the surrounding topography due to the large (~several km) altimeter footprint. Using the nominal footprint of Envisat over the flat water surface with a diameter of 2.5 km (red circles in Figure 2), only the radar returns that are over the wetlands are first considered (Figure 2). To identify the radar returns from the water surface, the 18-Hz ICE-1 backscattering coefficients are examined over the 18-Hz locations selected. Figure 3 shows the variations of the backscattering coefficients in 2004, and it is evident that the backscattered energy is generally higher over the main river stream than the surrounding agricultural field. It is clear that the backscattering coefficients are higher during spring and lower during autumn, which may indicate the spring flood due to the snow melt. We select the 18-Hz radar returns which have the backscattering coefficient higher than 20 dB, and spatially average them to construct the water level change time series

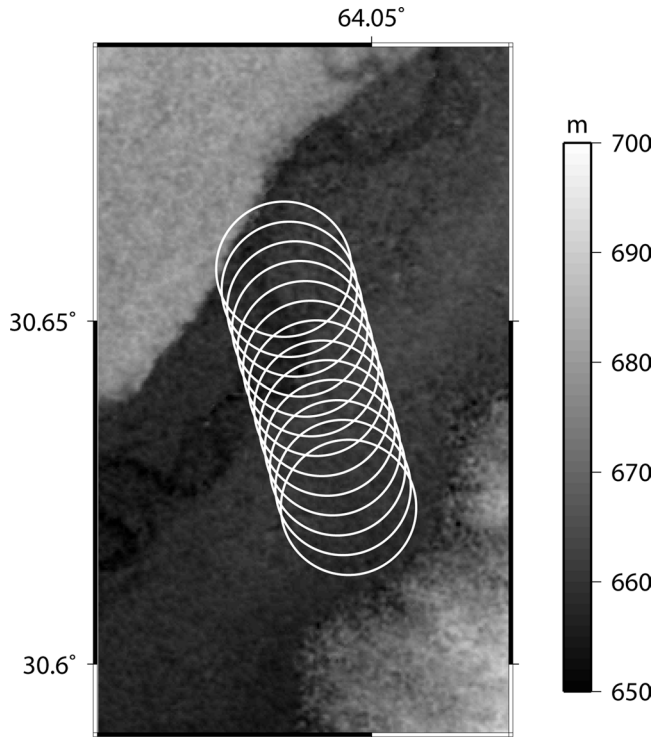


Figure 2. White circles denote the nominal footprints of the Envisat altimeter with a diameter of ~ 2.5 km along the 18-Hz nominal ground tracks of pass 253 over the Helmand River wetlands. Background is the SRTM DEM.

from September 2002 to July 2008 (Figure 4a). The seasonal variation with amplitude up to 10 m is obvious. The stage maxima occur in spring whereas the minima can be observed during autumn. Although there is no contemporary level gauge record to be compared with the water level variation from Envisat, this seasonal variation can also be observed in Figure 4b, which is from the discharge record from 1957 to 1969 obtained from a U.S. Geological Survey (USGS) river gauge station (Figure 1).

4.2. InSAR

The differential interferogram is generated after the topographic phase is simulated and removed using the 30-m resolution SRTM DEM. PALSAR FBS mode SAR images have a slant range pixel spacing of 4.7 m (7.5 m in ground range) and an azimuth pixel spacing of 3.2 m, and PALSAR FBD mode has a range pixel spacing of 9.4 m (ground range of 15 m) and an azimuth pixel spacing of 3.2 m. PALSAR FBD images are resampled to the pixel size of FBS images (Sandwell et al. 2008). A multiple-look factor of 1 by 2 is applied, so the interferogram pixel size represents an area of about 7.5 m by 6.4 m on ground. Moderate Goldstein adaptive filtering is applied to reduce the interferogram noise (Goldstein and Werner 1998).

Figures 5a and 6a show two examples of differential interferograms. It can be seen that the mountains, bare soils, and agricultural fields have low (0.2–0.5), high (0.7–0.9), and

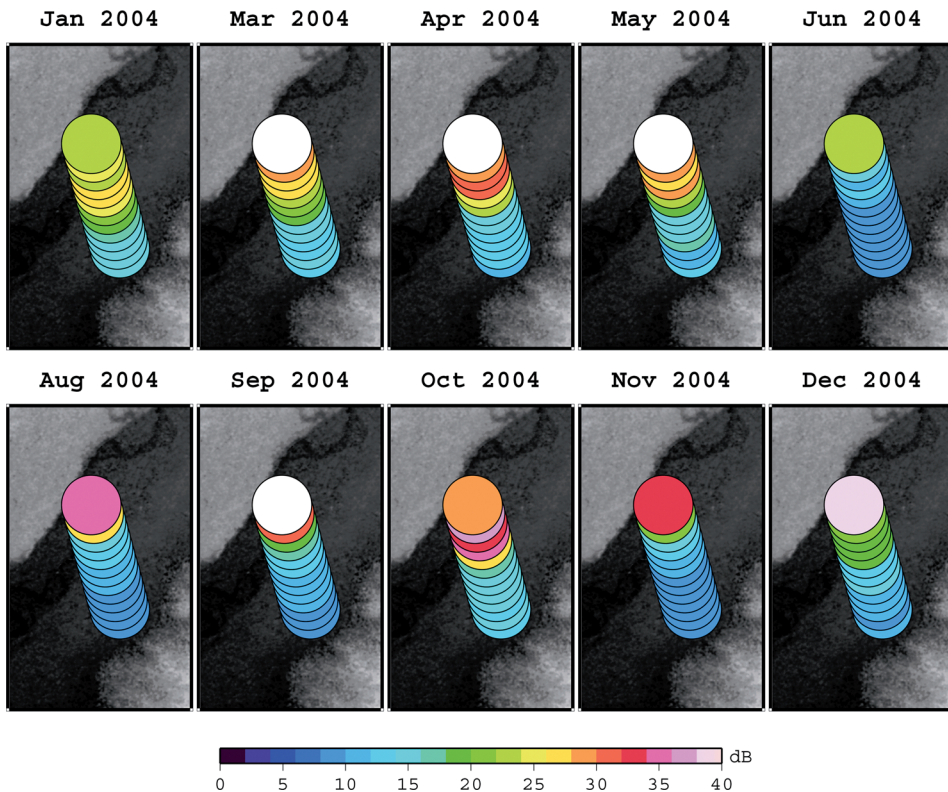


Figure 3. Examples of the 18-Hz ICE-1 backscattering coefficients (dB) (coded in color) along the 18-Hz satellite nominal ground tracks in 2004. The size of the circles approximately represents the size of the nominal altimeter footprint. The geographic coverage is the same as the one shown in Figure 2. (Figure appears in color online.)

intermediate (0.4–0.8) coherence values, respectively. It can also be seen from Figures 5b and 6b that the patches of high coherence pixels also exist in the marshes near the Helmand River. Because there is no detailed land cover map over the study area, classification on marsh, agricultural field, bare soil, and river is conducted using optical images from Google Earth (Figures 5c and 6c) and SAR intensity images. Only three of the processed InSAR pairs (pairs 2, 9, and 17 in Table 1) show high coherence (0.7) over most of the marshes, and the phase values of high coherence pixels within the marshes, over which the Envisat passes, are averaged. Using the water level changes measured from the Envisat altimeter, the integer ambiguity in an interferogram (Eq. (2)) can be resolved, and the interferogram can be unwrapped to resolve the absolute phase changes over other high coherence pixels. From the three highly coherent interferograms generated in this study, we do not see significant variations in the interferometric phase value. This suggests that the water level changes are relatively homogeneous over the study area. In contrast, a parallel study over southeastern Louisiana shows dynamic, spatially varying water level changes over wetlands (Kim et al. 2009). In that study, the Envisat altimeter data are used to resolve the absolute water level changes over the overlap of InSAR and altimeter measurements. The InSAR phase values are then used to map absolute water level changes across coherent pixels of interferograms.

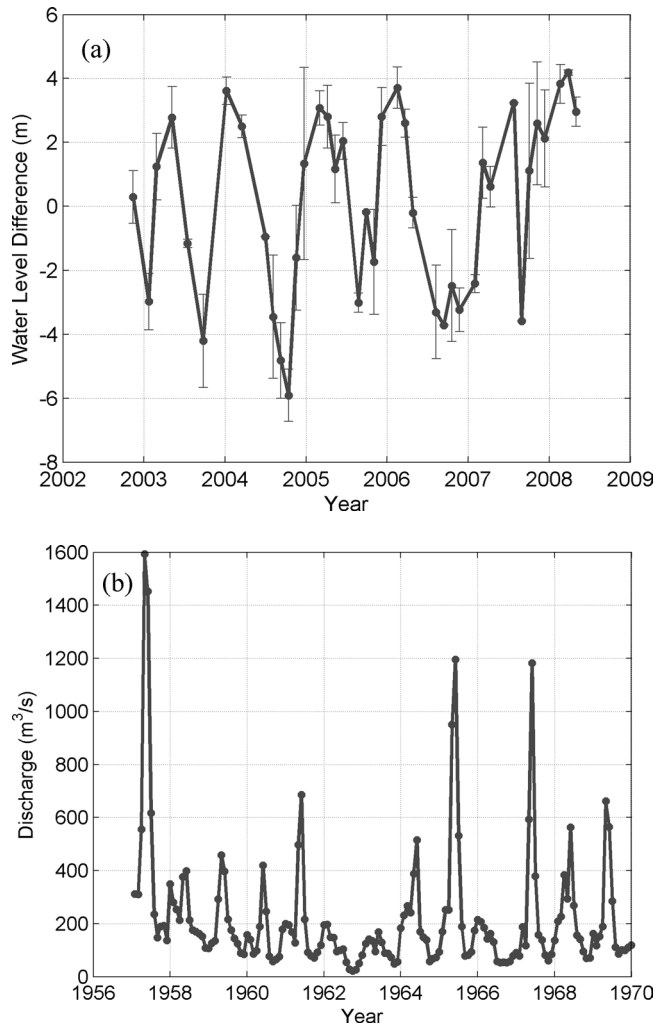


Figure 4. (a) Water level change (Δh) time series obtained from Envisat pass 253. (b) Discharge records estimated from the USGS river gauge station (http://nwis.waterdata.usgs.gov/nd/nwis/nwisman/?site_no=310800064110000) of which location is shown in Figure 1.

Statistics of the measured phase values and the estimated integer ambiguities over the marshes covered by the Envisat altimeter are shown in Table 2. From the estimated integer ambiguities, the absolute water level changes can be computed, and Figure 7 illustrates the water level changes from the Envisat altimeter and InSAR integrated with the altimeter over the Helmand River. The correlation coefficient and root-mean-square (RMS) difference between the altimeter and InSAR/altimeter integration are 0.97 and 6.79 cm, respectively.

It is known that InSAR images alone cannot observe absolute water level changes (Lu and Kwoun 2008). The reason is that InSAR phase values, which are ambiguously measured modulo by 2π , only represent the relative water level changes. In a simple case, for example, let us assume the water level over a wetland moves up or down by a

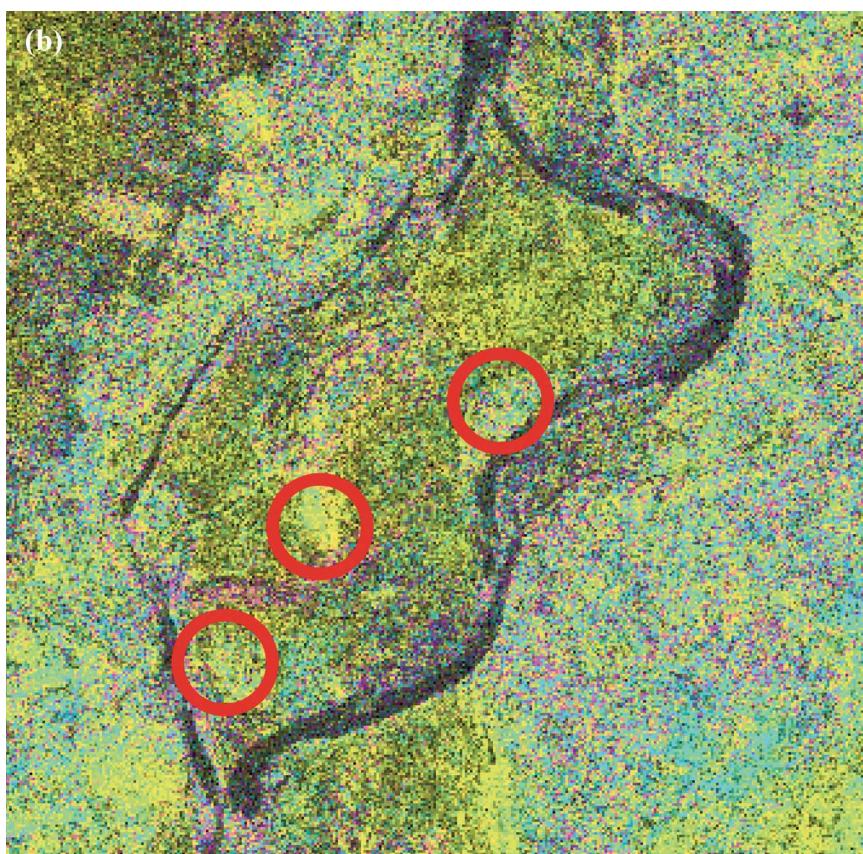
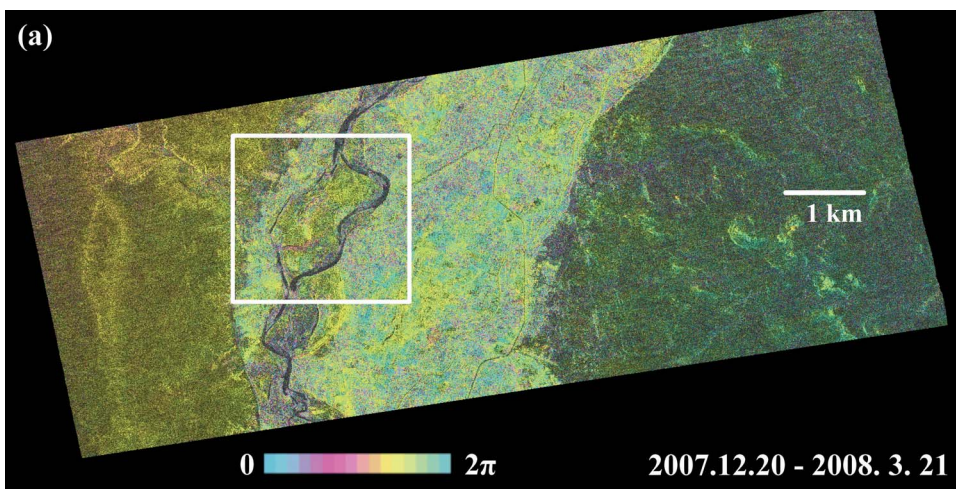


Figure 5. (a) Differential interferogram from the Cropped SAR images (2007.12.20–2008.3.21). (b) Enlarged differential interferogram. Red circles denote high coherence points within the marsh region. (c) Google Earth image. Red circles illustrate the marsh region. (Figure appears in color online.) (Continued)



Figure 5. (Continued)

constant height. The volumetric change of the wetland water storage can be calculated by the area of the wetland and the constant water level change. However, an InSAR image can only exhibit a constant phase shift with an ambiguity of multiples of 2π . This can be mistakenly interpreted as being no water level changes. To estimate the volumetric change of water storage, the absolute water level change at a single location within a wetland

Table 2

Averages and standard deviations of the measured phase value, and the integer ambiguities estimated using the absolute water level change from Envisat

Pair	$\bar{\phi}_{frac}$ (rad)	$\sigma_{\phi_{frac}}$ (rad)	\hat{N} (Integer ambiguity)
2007.12.20–2008.3.21	-7.6	1.301	-2
2008.2.21–2008.4.7	4.3	0.216	0
2008.2.9–2008.5.11	3.44	0.082	1

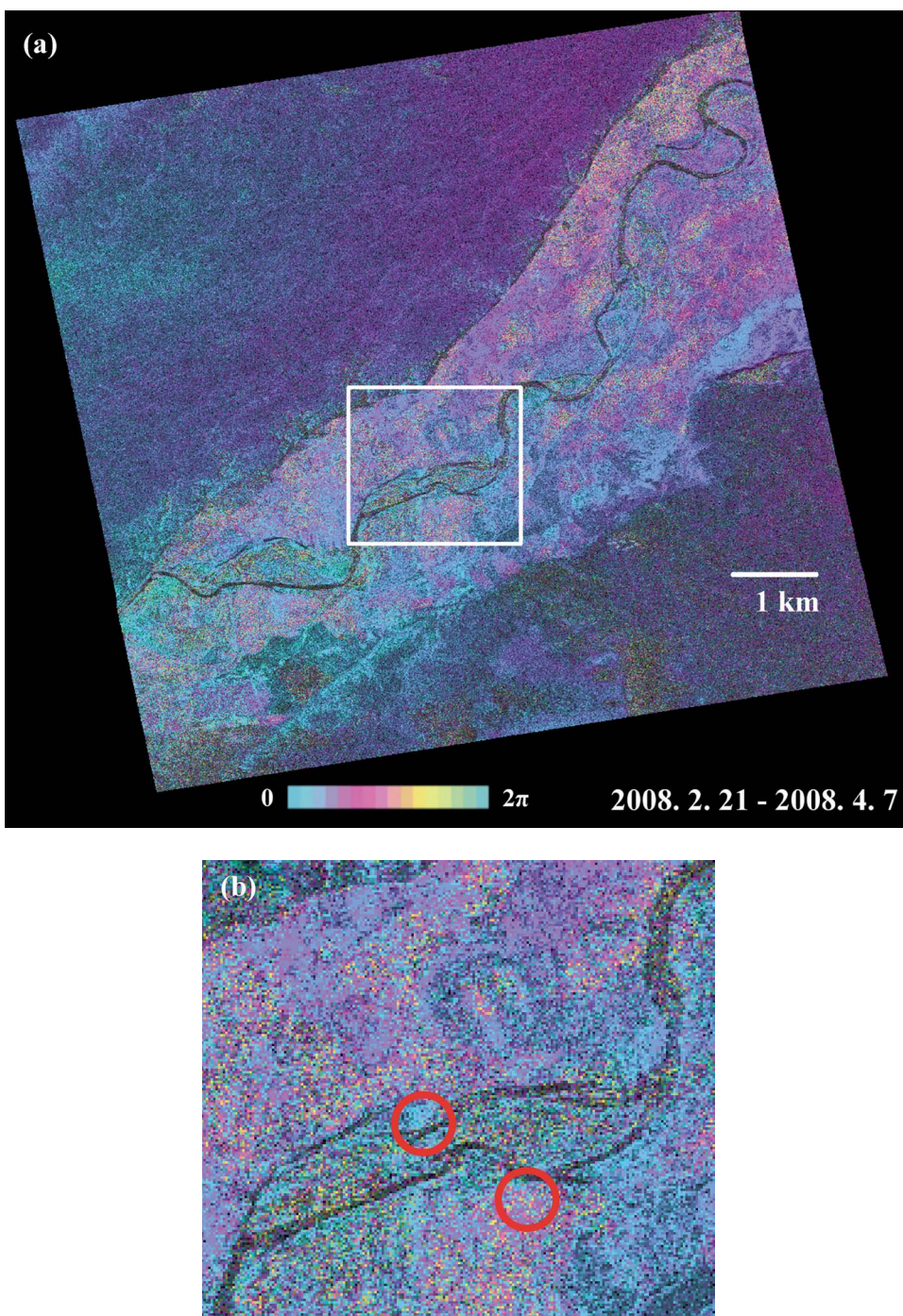


Figure 6. (a) Differential interferogram from the cropped SAR images (2008.2.21–2008.4.7). (b) Enlarged differential interferogram. Red circles denote high coherence points within the marsh region. (c) Google Earth image. Red circles illustrate the marsh region. (Figure appears in color online.) (Continued)



Figure 6. (Continued)

body is required. What we have demonstrated in this study is that the altimeter can be used to correct the phase ambiguities in InSAR images to estimate the absolute water level changes. Then, the “calibrated” interferogram phase values can be used to calculate the absolute water level changes over other high-coherence areas as long as they can be successfully unwrapped. The estimated absolute water level changes from the integration of altimeter and InSAR can provide a valuable hydrologic dataset over a region such as Afghanistan, where no in situ measurements exist or where they are unavailable to the public.

The accuracy of altimeter measurements for this purpose does not need to be very high. In principle, as SAR is a side-looking sensor, an accuracy to the $\lambda/(2\cos\theta_{inc})$ is sufficient. For ALOS PALSAR with $\lambda = 23.6$ cm and $\theta_{inc} = 38^\circ$, this corresponds to about 15 cm.

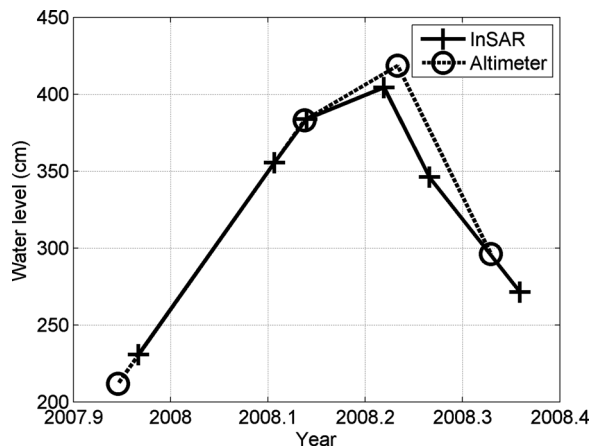


Figure 7. Comparison of the absolute surface water elevations over the Helmand River obtained from the Envisat and the integration of the Envisat altimeter and InSAR measurements.

5. Conclusions

An innovative technique to build the absolute water level change map using Envisat radar altimetry and ALOS PALSAR InSAR in the Helmand River wetlands was developed and demonstrated. The 18-Hz regional stackfile method is used to construct the absolute water level change from the retracked Envisat measurements, and they are used as a reference surface to resolve the integer ambiguity in the wrapped interferogram and to obtain absolute water level changes within the marsh region. The integration of altimeter and InSAR enables the monitoring of absolute water level changes over the Helmand River basin in Afghanistan, of which any recent hydrological data are not released. The technique of retrieving the absolute water change from the integration of altimetry and InSAR is being explored in other wetlands to test the applicability of the proposed methodology.

Acknowledgments

This research is partially supported by grants from the National Geospatial-Intelligence Agency's University Research Initiatives Program, HM1582-07-1-2024; the Climate, Water, and Carbon Program at the Ohio State University; and the U.S. Geological Survey Land Remote Sensing Program. PALSAR data are copyrighted by JAXA/METI 2006–2008 and are provided by ASF. Envisat radar altimetry data are provided by ESA/ESRIN. We also thank two anonymous reviewers for their constructive comments which have improved the manuscript.

References

- Alsdorf, D. E., J. M. Melack, T. Dunne, L. Mertes, L. Hess, and L. C. Smith. 2000. Interferometric radar measurements of water level changes on the Amazon floodplain. *Nature* 404:174–177.
- Alsdorf, D. E., L. C. Smith, and J. M. Melack. 2001. Amazon floodplain water level changes measured with interferometric SIR-C radar. *IEEE Trans. Geosci. Remote Sensing* 39:423–431.
- Bamber, J. L. 1994. Ice sheet altimeter processing scheme. *Int. J. Remote. Sens.* 15:925–938.
- Benveniste, J., Ed. 2002. *ENVISAT RA-2/MWR product handbook, European Space Agency Report PO-TN-ESR-RA-0050*. Noorwijk, The Netherlands: European Space Agency.
- Berry, P. A.M., J. D. Garlick, J. A. Freeman, and E. L. Mathers. 2005. Global inland water monitoring from multi-mission altimetry. *Geophys. Res. Lett.* 32:L16401, doi: 10.1029/2005GL022814.
- Birkett, C. M. 1995. The contribution of TOPEX/POSEIDON to the global monitoring of climatically sensitive lakes. *J. Geophys. Res.* 100:25179–25204.
- Birkett, C. M. 1998. Contribution of the TOPEX NASA radar altimeter to the global monitoring of large rivers and wetlands. *Water Resour. Res.* 34:1223–1239.
- Birkett, C. M., L. A.K. Mertes, T. Dunne, M. H. Costa, and M. J. Jasinski. 2002. Surface water dynamics in the Amazon Basin: Application of satellite radar altimetry. *J. Geophys. Res.* 107, doi: 10.1029/2001JD000609.
- Frappart, F., S. Calmant, M. Cauhopé, F. Seyler, and A. Cazenave. 2006. Preliminary results of ENVISAT RA-2-derived water levels validation over the Amazon basin. *Remote Sens. Environ.* 100:252–264.
- Goldstein, R. M., and C. L. Werner. 1998. Radar interferogram filtering for geophysical applications. *Geophys. Res. Lett.* 25:4035–4038.
- Integrated Regional Information Networks (IRIN). 2005. Afghanistan: Flood relief under way. <http://www.irinnews.org/report.aspx?reportid=28344>
- Kim, J. W., Z. Lu, H. Lee, C. K. Shum, C. Swarzenski, T. Doyle, and S. Baek. 2009. Integrated analysis of PALSAR/Radarsat-1 InSAR and ENVISAT altimeter for mapping of absolute water level changes in Louisiana wetland. *Remote Sens. Environ.*, doi: 10.1016/j.rse.2009.06.014.

- Lee, H., C. K. Shum, Y. Yi, A. Braun, and C. Y. Kuo. 2008. Laurentia crustal motion observed using TOPEX/POSEIDON radar altimetry. *J. Geodyn.* 46:182–193, doi: 10.1016/j.jog.2008.05.001.
- Lee, H., C. K. Shum, Y. Yi, M. Ibaraki, J.-W. Kim, A. Braun, C.-Y. Kuo, and Z. Lu. 2009. Louisiana wetland water level monitoring using retracked TOPEX/POSEIDON altimetry. *Marine Geodesy*, 284–302.
- Lu, Z., and O.-I. Kwoun. 2008. Radarsat-1 and ERS InSAR analysis over southeastern coastal Louisiana: Implications for mapping water-level changes beneath swamp forests. *IEEE Trans. Geosci. Remote Sensing* 46:2167–2184.
- Lu, Z., M. Crane, O.-I. Kwoun, C. Wells, C. Swarzenski, and R. Rykhus. 2005. C-band radar observes water level change in swamp forests. *EOS* 86:141–144.
- Morris, C. S., and S. K. Gill. 1994. Evaluation of the TOPEX/POSEIDON altimeter system over the Great Lakes. *J. Geophys. Res.* 99:24527–24539.
- ReliefWeb. 2003. Afghanistan: Flood victims continue to suffer despite emergency response. <http://www.reliefweb.int/rw/rwb.nsf/AllDocsByUNID/498d7e06efe3f43185256d1000523396>
- Sandwell, D. T., D. Myer, R. Mellors, M. Shimada, B. Brooks, and J. Foster. 2008. Accuracy and resolution of ALOS interferometry: Vector deformation maps of the Father's Day intrusion at Kilauea. *IEEE Trans. Geosci. Remote Sensing* 46:3524–3534.
- Vining, K. C., and A. V. Vecchia. 2007. Water-balance simulations of runoff and reservoir storage for the Upper Helmand watershed and Kajakai Reservoir, central Afghanistan. *U.S. Geological Survey Scientific Investigations Report* 2007–5148.
- Wdowinski, S., F. Amelung, F. Miralles-Wilhelm, T. Dixon, and R. Carande. 2004. Space-based measurements of sheet-flow characteristics in the Everglades wetland, Florida. *Geophys. Res. Lett.* 31:L15503, doi: 10.1029/2004GL020383.
- Williams-Sether, T. 2008. Streamflow characteristics of streams in the Helmand Basin, Afghanistan. *U.S. Geological Survey Data Series* 333.